Models of the Cytochromes. Axial Ligand Orientation and Complex Stability in Iron(II) Porphyrinates: The Case of the Noninteracting d_π Orbitals

Martin K. Safo,[1a,b] Marlys J. M. Nesset,[1c] F. Ann Walker,*[,1c] Peter G. Debrunner,*[,1d] and W. Robert Scheidt*[,1a]

Contribution from the Department of Chemistry and Biochemistry, University of Notre Dame, Notre Dame, Indiana 46556, Department of Chemistry, University of Arizona, Tucson, Arizona 85721, and Department of Physics, University of Illinois, Urbana, Illinois 61801

Received May 14, 1997[⊗]

Abstract: The synthesis and characterization of seven bis-pyridine and bis-imidazole complexes of iron(II) tetramesitylporphyrinate are reported. X-ray crystal structures of three of the complexes, [Fe(TMP)(4-CNPy)$_2$], [Fe(TMP)(3-CNPy)$_2$], and [Fe(TMP)(4-MePy)$_2$], have been solved and all show parallel axial ligand orientations with nearly planar porphyrinato cores. The Mössbauer spectra of six of the complexes, having pyridine ligands with pK_a(PyH$^+$) ranging from ∼1.1 (4-CNPy) to 9.7 (4-NMe$_2$Py), have been determined. The Mössbauer isomer shifts at 120 K are in the range of 0.36−0.45 mm/s, and the quadrupole splittings (ΔE_Q) are in the range of 1.11−1.27 mm/s. Thus, unlike the corresponding Fe(III) complexes, the X-ray structures and Mössbauer spectroscopic parameters of these (tetramesitylporphyrinato)iron(II)−bis(pyridine) complexes are shown to be essentially independent of the basicity and π donor/acceptor properties of the axial pyridine ligands. These solid-state structural and spectroscopic properties are compared to the thermodynamic properties of the same series of complexes in solution (Nesset, M. J. M.; Shokhirev, N. V.; Enemark, P. D.; Jacobson, S. E.; Walker, F. A. *Inorg. Chem.* **1996**, *35*, 5188): The equilibrium constants, β_2^{II}, for binding two ligands to [Fe^{II}(TMP)(DMF)] are also nearly independent of the basicity of the axial pyridine ligand, although the Fe^{III}/Fe^{II} reduction potentials vary strongly with ligand basicity due to the large variation in β_2^{III}, the equilibrium constant for binding two ligands to the Fe(III) complex. Hence, it appears that low-spin d^6 metalloporphyrins have a marked preference for parallel orientation of planar axial ligands, and that the charge asymmetry at the iron nucleus (deduced from Mössbauer quadrupole splittings) and the thermodynamics of ligand binding are unaffected by the electronic properties of the axial ligand. The major reason for the marked preference for parallel ligand orientation for iron(II) porphyrinates appears to be lack of a means of energy stabilization of the ruffled core of the perpendicular orientation.

Introduction

Model hemes based on iron(II) and iron(III) tetraphenylporphyrinates have found considerable utility in elucidating and understanding the properties of the heme proteins.[2] However, these synthetic hemes often introduce new or different properties that the investigator may not have considered beforehand, for example, rapid rotation of axial ligands in homogeneous solution.[3−8] In comparison to the axial ligands in model hemes, rotation of the axial ligands of heme proteins is prevented because they are linked by side chains that are covalently attached to the protein backbone. The orientations of planar ligands provided by the protein are also tightly controlled by protein structural constraints that include steric crowding of other protein side chains very near the heme and, in the case of histidine ligands, hydrogen bonding of the NH group of the imidazole ring to either amide carbonyl groups of the protein backbone or, possibly, hydrogen bond acceptors provided as amino acid side chains. Physiologically relevant ligands provided by the protein include the imidazole side chain of histidine,[9,10] the methyl thioether side chain of methionine,[10] the thiolate of cysteine,[11] the phenolate of tyrosine,[11] and in the case of cytochrome *f*,[12] the N-terminal amino group of the polypeptide.

For the case of heme centers coordinated to two planar imidazole ligands of histidine residues, two limiting orientations of the axial ligand planes have been implicated in the structures of the cytochromes: imidazole planes oriented parallel to each other (cytochromes b_5,[9] three of the heme centers of cytochromes c_3,[13] the *b* hemes of sulfite oxidase[14] and flavocytochrome b_2,[15] and the heme *a* of cytochrome oxidase[16]), while other bis-histidine-coordinated heme proteins are believed to have their axial imidazole planes orientated perpendicular to

⊗ Abstract published in *Advance ACS Abstracts,* September 15, 1997.

(1) (a) University of Notre Dame. (b) Present address: Department of Medicinal Chemistry, Medical College of Virginia (VCU), P.O. Box 540, Richmond, VA 23298. (c) University of Arizona. (d) University of Illinois.

(2) Walker, F. A.; Simonis, U. Iron−Porphyrin Chemistry. In *Encyclopedia of Inorganic Chemistry*; Berliner, L. J., Reuben, J., Eds.; Plenum: New York, 1993; pp 133−274.

(3) Nakamura, M.; Groves, J. T. *Tetrahedron* **1984**, *44*, 3225.

(4) Walker, F. A.; Simonis, U. *J. Am. Chem. Soc.* **1991**, *113*, 8652.

(5) Shokhirev, N. V.; Shokhireva, T. Kh.; Polam, J. R.; Watson, C. T.; Raffii, K.; Simonis, U.; Walker, F. A. *J. Phys. Chem. A* **1997**, *101*, 2778.

(6) Momot, K. I.; Walker, F. A. *J. Phys. Chem. A* **1997**, *101*, 2787.

(7) Nakamura, M.; Tajima, K.; Tada, K.; Ishizu, K.; Nakamura, N. *Inorg. Chim. Acta* **1994**, *224*, 113.

(8) Polam, J. R.; Shokhireva, T. Kh.; Raffii, K.; Simonis, U.; Walker, F. A. *Inorg. Chim. Acta* In press.

(9) Mathews, F. A.; Czerwinski, E. W.; Argos, P. In *The Porphyrins*; Dolphin, D., Ed.; Academic Press: New York, 1979; Vol. VII, pp 107−147.

(10) Dickerson, R. E.; Takano, T.; Eisenberg, D.; Kallai, O. B.; Samson, L.; Cooper, A.; Margoliash, E. *J. Biol. Chem.* **1971**, *246*, 1971.

(11) Poulos, T. L. In *Cytochrome P-450: Structure, Mechanism, and Biochemistry*; Ortiz de Montellano, P. R., Ed.; Plenum: New York, 1986; pp 505−523.

(12) Martinez, S. E.; Huang, D.; Szczepaniak, A.; Cramer, W. A.; Smith, J. L. *Structure* **1994**, *2*, 95.

(13) (a) Pierrot, M.; Haser, R.; Frey, M.; Payan, F.; Astier, J.-P. *J. Biol. Chem.* **1982**, *257*, 14341. (b) Higuchi, Y.; Kusunoki, M.; Matsuura, Y.; Yasuoka, N.; Kakudo, M. *J. Mol. Biol.* **1984**, *172*, 109.

(14) Kipke, C. A.; Cusanovich, M. A.; Tollin, G.; Sunde, R. A.; Enemark, J. H. *Biochemistry* **1988**, *27*, 2918.

S0002-7863(97)01565-5 CCC: $14.00

each other. Proteins of the latter group have been identified largely on the basis of spectroscopic data for the oxidized (Fe(III)) forms, and include the *b* hemes of mitochondrial complex III, also known as cytochrome bc_1,[17] the similar *b* hemes of cytochrome b_6f of chloroplasts, one of the *c*-type hemes of cytochrome c_3,[13] and the *c*-type heme of cytochrome *c″* of *Methylophilus methylotrophus*.[18]

Based on structural and spectroscopic investigations of the bis(2-methylimidazole) complex of (tetraphenylporphyrinato)-iron(III), $[TPPFe(2\text{-}MeHIm)_2]^+$,[19,20] we concluded some time ago that for low-spin d^5 ferriheme centers, parallel orientation of axial ligands is energetically favored, and that either bulky axial ligands, such as 2-methylimidazole (or, as we later found, the combination of tetrakis(2,6-disubstituted phenyl)porphyrinates together with pyridines[21,22] or bulky imidazoles[23]), are required to force the perpendicular relative orientation of planar axial ligands in Fe(III) porphyrinates. We also proposed that the reduction potentials of bis-histidine-ligated cytochromes might in part be determined by the orientation of the axial ligand planes, with perpendicular orientation creating the more positive reduction potential.[16] This appeared to be consistent with the observation that the membrane-bound bis-histidine-coordinated *b* cytochromes of the bc_1 and b_6f complexes, whose single-feature EPR spectra suggest that the imidazole planes are perpendicularly oriented,[17] tend to have more positive reduction potentials[17b,24] than those for which the EPR signals are rhombic[25] and the structures are known or believed to have parallel-oriented imidazole planes.[9] Inherent in this hypothesis is the belief that no change would take place in histidine imidazole plane orientation when electron transfer occurred, and hence both Fe(III) and Fe(II) forms of each limiting type of cytochrome would have the same ligand orientations. This is known to be the case for some of the small, water-soluble cytochromes such as cytochrome b_5[9] and *c*,[10] but has not yet been elucidated for the membrane-bound *b* cytochromes.

During the time over which our studies of bis(hindered imidazole) and -(pyridine) complexes of Fe(III) porphyrinates were being carried out and the above-described hypothesis was developed, we had assumed that for the closed subshell configuration of low-spin d^6 Fe(II) porphyrinates, planar axial ligands would prefer to align themselves in mutually perpendicular planes, to maximize the π-bonding interactions between the filled d_π orbitals of Fe(II) and the π^* orbitals of the ligands. However, the investigations reported herein, which involve structural, spectroscopic, and thermodynamic measurements of bis(pyridine) complexes of (tetramesitylporphyrinato)iron(II), clearly show that low-spin Fe(II) porphyrinates strongly prefer to have planar axial ligands oriented parallel to each other, and that π-bonding interactions between Fe(II) and the axial ligands are minimal. Herein we report the structures of three complexes, $[Fe(TMP)(4\text{-}CNPy)_2]$, $[Fe(TMP)(3\text{-}CNPy)_2]$, and $[Fe(TMP)(4-MePy)_2]$, and the Mössbauer parameters of a series of $Fe^{II}(TMP)$ complexes with pyridines of widely varying basicities, where, in all cases, the analogous $Fe^{III}(TMP)$ derivative is known to have mutually perpendicular axial ligands.[21,22] The solid state properties of these ferrocytochrome models will then be compared to the thermodynamic properties of the same complexes in homogeneous solution (reduction potentials of the Fe^{III}/Fe^{II} couples and the equilibrium constants for binding the axial ligands to Fe(II) TMP at ambient temperatures).[26] Possible reasons for and consequences of the lack of sensitivity of low-spin Fe(II) porphyrinate bis-ligand complexes to the σ-donor and π-donor/acceptor properties of the axial ligands will be evaluated.

Experimental Section

General Information. Reactions were performed with solvents distilled under argon prior to use. THF and benzene were distilled from sodium benzophenone ketyl. Dichloromethane, chloroform, and hexane were distilled from CaH_2. 4-Cyanopyridine was recrystallized from CH_2Cl_2. Other imidazole and pyridine ligands were obtained from Aldrich and used without further purification. Tetramesitylporphyrin was prepared by slight modification of the procedures by Lindsey *et al.*,[27] and as described previously.[21] The [Fe(TMP)(OH)] was prepared by shaking a CH_2Cl_2 solution of [Fe(TMP)Cl] with a 2 M solution of KOH. The reduced iron complex, [Fe(TMP)], was prepared by reducing a benzene solution of [Fe(TMP)(OH)] with ethanethiol or a chloroform solution with Zn(Hg). Solid [Fe(TMP)] precipitated from the benzene solution. UV−vis (benzene): Split soret 419.0, 430.2; α and β bands 527.5, 562.9 nm. This [Fe(TMP)] was immediately used for synthesis of the bis-pyridine complexes.

Mössbauer samples were prepared as mulls in Apiezon L grease. Mössbauer measurements were made at 4.2 and/or 120 K on a constant-acceleration spectrometer. The spectra were fitted with two Lorentzians of equal area. Isomer shifts are quoted relative to metallic iron at room temperature. UV−visible spectra were recorded on a Perkin-Elmer Lambda 4C spectrophotometer.

Synthesis of [Fe(TMP)(4-CNPy)$_2$]. A chloroform solution (15 mL) of [Fe(TMP)] prepared by reduction of [Fe(TMP)(OH)] (130 mg, 0.150 mmol) with Zn(Hg) was transferred by cannula filtration into a Schlenk flask containing the 4-cyanopyridine ligand (300 mg, 2.88 mmol). The reaction mixture was shaken for a minute, and then layered with hexane for crystallization. X-ray quality crystals formed after 5 days. UV−vis ($CHCl_3$) λ_{max} (log ϵ): 421.0 (5.09), 527.2 (4.16), 558.0 (4.03) nm.

Synthesis of [Fe(TMP)(3-CNPy)$_2$]. A chloroform solution (15 mL) of [Fe(TMP)] prepared by reduction of [Fe(TMP)(OH)] (80 mg, 0.080 mmol) with Zn(Hg) was cannula-filtered into a Schlenk flask containing the 3-cyanopyridine ligand (250 mg, 2.40 mmol). The reaction mixture

(15) (a) Xia, Z.-X.; Shamala, N.; Bethge, P. H.; Lim, L. W.; Bellamy, H. D.; Xuong, N. H.; Lederer, F.; Mathews, F. S. *Proc. Natl. Acad. Sci. U.S.A.* **1987**, *84*, 2629. (b) Dubois, J.; Chapman, S. K.; Mathews, F. S.; Reid, G. A.; Lederer, F. *Biochemistry* **1990**, *29*, 6393.

(16) Iwata, S.; Ostermeier, C.; Ludwig, B.; Michel, H. *Nature* **1995**, *376*, 660.

(17) (a) Salerno, J. C. *J. Biol. Chem.* **1984**, *259*, 2331. (b) Tsai, A.; Palmer, G. *Biochim. Biophys. Acta* **1982**, *681*, 484. (c) Tsai, A.-H.; Palmer, G. *Biochim. Biophys. Acta* **1983**, *722*, 349.

(18) (a) Berry, M. J.; George, S. J.; Thomson, A. J.; Santos, H.; Turner, D. L. *Biochem. J.* **1990**, *270*, 413. (b) Costa, H. S.; Santos, H.; Turner, D. L.; Xavier, A. V. *Eur. J. Biochem.* **1992**, *208*, 427. (c) Costa, H. S.; Santos, H.; Turner, D. L. *Eur. J. Biochem.* **1993**, *215*, 817.

(19) Walker, F. A.; Huynh, B. H.; Scheidt, W. R.; Osvath, S. R. *J. Am. Chem. Soc.* **1986**, *108*, 5288.

(20) Abbreviations used: Axial ligands: 2-MeHIm, 2-methylimidazole; 1,2-Me_2Im, 1,2-dimethylimidazole; 1-MeIm, 1-methylimidazole; 1-VinIm, 1-vinylimidazole; 1-BzylIm, 1-benzylimidazole; 4-CNPy, 4-cyanopyridine; 3-CNPy, 3-cyanopyridine; 3-ClPy, 3-chloropyridine; 4-MePy, 4-methylpyridine; Py, pyridine; 4-NMe_2Py, 4-(dimethylamino)pyridine; PMe_3, trimethylphosphine; DMF, dimethylformamide. Porphyrins: TMP, tetramesitylporphyrin; TPP, tetraphenylporphyrin; $(2,6\text{-}Cl_2)_4$TPP, tetrakis(2,6-dichlorophenyl)porphyrin; $(2,6\text{-}Br_2)_4$TPP, tetrakis(2,6-dibromophenyl)porphyrin; $(2,6\text{-}F_2)_4$TPP, tetrakis(2,6-difluorophenyl)porphyrin; $(2,6\text{-}(OMe)_2)_4$TPP, tetrakis(2,6-dimethoxyphenyl)porphyrin; OEP, octaethylporphyrin. Other: N_p, porphinato nitrogen; MM2, molecular mechanics program; β_2^{II}, equilibrium constant for binding two axial ligands to iron(II) porphyrinates; β_2^{III}, equilibrium constant for bidning two axial ligands to iron(III) porphyrinates.

(21) Safo, M. K.; Gupta, G. P.; Walker, F. A.; Scheidt, W. R. *J. Am. Chem. Soc.* **1991**, *113*, 5497.

(22) Safo, M. K.; Gupta, G. P.; Watson, C. T.; Simonis, U.; Walker, F. A.; Scheidt, W. R. *J. Am. Chem. Soc.* **1992**, *114*, 7066.

(23) Munro, O. Q.; Marques, H. M.; Debrunner, P. G.; Mohanrao, K.; Scheidt, W. R. *J. Am. Chem. Soc.* **1995**, *117*, 935.

(24) von Jagow, G.; Engel, W. D. *Angew. Chem., Int. Ed. Engl.* **1980**, *19*, 659.

(25) Rivera, Barillas-Mury, C.; Christensen, K. A.; Little, J. W.; Wells, M. A.; Walker, F. A. *Biochemistry* **1992**, *31*, 12233 and references therein.

(26) Nesset, M. J. M.; Shokhirev, N. V.; Enemark, P. D.; Jacobson, S. E.; Walker, F. A. *Inorg. Chem.* **1996**, *35*, 5188.

(27) Watner, R. W.; Lawrence, D. S.; Lindsey, J. S. *Tetrahedron Lett.* **1987**, *28*, 3069. Lindsey, J. S.; Wagner, R. W. *J. Org. Chem.* **1988**, *54*, 828.

Table 1. Summary of Crystal Data and Intensity Collection Parameters

complex	$[Fe(TMP)(4\text{-}CNPy)_2]\cdot 2CHCl_3$	$[Fe(TMP)(4\text{-}MePy)_2]\cdot 2C_6H_6$	$[Fe(TMP)(3\text{-}CNPy)_2]\cdot 2CHCl_3$
formula	$FeCl_6N_8C_{70}H_{62}$	$FeN_8C_{80}H_{78}$	$FeCl_6N_8C_{70}H_{62}$
fw, amu	1283.88	1179.39	1283.88
space group	$P\bar{1}$	$P\bar{1}$	$P\bar{1}$
T, K	124	124	124
a, Å	10.632(4)	10.556(2)	10.135(2)
b, Å	12.742(4)	11.188(2)	12.326(2)
c, Å	13.722(5)	13.972(2)	13.562(2)
α, deg	97.38(3)	90.93(1)	106.46(1)
β, deg	105.82(3)	102.66(2)	96.54(1)
γ, deg	107.92(3)	94.64(2)	102.78(2)
Z	1	1	1
R_1	0.070	0.059	0.062
R_2	0.090	0.078	0.073
goodness of fit	2.321	2.350	3.084

was shaken for a minute, and then layered with hexane for crystallization. X-ray quality crystals formed after 4 days.

Synthesis of [Fe(TMP)(4-MePy)$_2$]. A benzene filtrate (30 mL) of [Fe(TMP)] prepared by reduction of [Fe(TMP)(OH)] with ethanethiol (after [Fe(TMP)] solid crystals had been harvested) was reacted with 4-methylpyridine (200 mg, 2.15 mmol). The reaction mixture was shaken for a minute, and then layered with hexane for crystallization. X-ray quality crystals formed after 6 days. UV−vis ($CHCl_3$) λ_{max}: 423.0, 530.0, 561.6 nm.

Synthesis of [Fe(TMP)(Py)$_2$]. [Fe(TMP)] (50 mg, 0.060 mmol, prepared by reduction of [Fe(TMP)(OH)] with ethanethiol) was stirred in chloroform solution with Zn(Hg) for 10 min. The solution was then transferred by cannula into a Schlenk flask containing the pyridine ligand (200 mg, 2.24 mmol). The reaction mixture was shaken for a minute, and then layered with hexane for crystallization. Crystals formed after 6 days. UV−vis ($CHCl_3$) λ_{max}: 422.0, 528.7, 559.8 nm.

[Fe(TMP)(4-NMe$_2$Py)$_2$], [Fe(TMP)(3-ClPy)$_2$], and **[Fe(TMP)(1-MeIm)$_2$]** were prepared as described for [Fe(TMP)(Py)$_2$]. Only microcrystalline material was obtained in each case. UV−vis data for the first and third complexes are λ_{max} 425.5, 536.5, 571.0 nm and 426.5, 536.9, 565.0 nm, respectively.

Structure Determinations. The three complexes [Fe(TMP)(4-CNPy)$_2$], [Fe(TMP)(3−CNPy)$_2$], and [Fe(TMP)(4-MePy)$_2$] were examined on an Enraf-Nonius CAD4 diffractometer equipped with a locally modified Syntex LT-1 low-temperature attachment on the diffractometer. Preliminary examination of crystals of the complexes at a temperature of 124 K led to a one-molecule triclinic cell in each case. Final cell constants and complete details of the intensity collection and least-squares refinement parameters for the complexes are summarized in Tables 1 and S1, Supporting Information. Precise cell constants were determined from least-squares refinement of 25 automatically centered reflections. Four standard reflections were monitored during each data collection for crystal movements and possible deterioration of the crystal. No significant decay was observed for any of the complexes.

Intensity data were reduced by using the data reduction program suite of R. H. Blessing.[28] All data with $F_o \geq 3.0\sigma(F_o)$ were retained as observed and used in all subsequent refinements. The centrosymmetric space group $P\bar{1}$ was assumed for all complexes; this choice was consistent with all subsequent developments of structure solution and refinement. All structures of the complexes were solved with the direct methods program MULTAN[29] and difference Fourier syntheses. The full-matrix least-squares programs ALLS or ORFLS were used for structure refinement. After several cycles of least-squares refinement, the possible hydrogen atoms were located in the complexes. The hydrogen atom positions were idealized and included in subsequent cycles of least-squares refinement as fixed contributors (C−H = 0.95 Å and $B(H) = 1.3 \times B(C)$, with additional reidealization as required. All atoms were refined anisotropically except hydrogens and some disordered (*vide infra*) non-hydrogen atoms.

In all three species, the six-coordinate complexes have required inversion symmetry with the iron at the inversion center. All complexes have a single disordered solvent molecule region. In the 4-CNPy complex, two separate chloroform molecule positions were included in the full-matrix least-squares refinements with atomic occupancies of 0.5 for all atoms in one chloroform group and 0.25 for the other. A third group was related to another chloroform molecule by an inversion center and was refined by rigid-group methods: A C−Cl distance of 1.74 Å with atomic occupancies of 0.1 was used. Final atomic coordinates can be found in Table S2, Supporting Information. In the 3-CNPy complex, the three chlorine atoms of the chloroform solvent were disordered over two orientations. All positions were included in the full-matrix least-squares refinements with atomic occupancies of 0.85 for all atoms in one group and 0.15 for the other. Final atomic coordinates can be found in Table S3, Supporting Information. In the 4-MePy complex, the benzene solvent molecule was disordered over two positions. These were included in the full-matrix least-squares refinement with atomic occupancies of 0.6 and 0.4 for atoms in the two respective groups. Final atomic coordinates can be found in Table S4, Supporting Information. Anisotropic temperature factors, fixed hydrogen atom positions, and group parameters for all three complexes are also given in the Supporting Information.

Results and Discussion

General. All the $Fe^{II}TMP$ complexes characterized and reported herein are low-spin six-coordinate complexes as indicated by UV−vis and/or Mössbauer spectroscopy, and/or single-crystal structure determination. The UV−vis spectral bands of all complexes are between 421−427 and 527−537 nm, with a shoulder at 558−571 nm, and are typical of other low-spin iron(II) tetraphenylporphyrinates,[30,31] a confirmation of the iron(II) oxidation state. The spectral bands of the low-basicity pyridine complexes are slightly blue shifted compared to the high-basicity pyridine and imidazole complexes.

Mössbauer Spectra. The Mössbauer parameters of the complexes of this study are given in Table 2 along with values for other low-spin iron(II) porphyrinates.[32−40] They are typical

(28) Blessing, R. H. *Crystallogr. Rev.* **1987**, *1*, 3.

(29) Programs used in this study included local modifications of Main, Hull, Lessinger, Germain, Declerq, and Woolfson's MULTAN, Jacobson's ALLS, Zalkin's FORDAP, Busing and Levy's ORFFE, and Johnson's ORTEP2. Atomic form factors were from: Cromer, D. T.; Mann, J. B. *Acta Crystallogr., Sect. A* **1968**, *A24*, 321. Real and imaginary corrections for anomalous dispersion in the form factor of the iron atom were from: Cromer, D. T.; Liberman, D. J. *J. Chem. Phys.* **1970**, *53*, 1891. Scattering factors for hydrogen were from: Stewart, R. F.; Davidson, E. R.; Simpson, W. T. *J. Chem. Phys.* **1965**, *42*, 3175. All calculations were performed on VAX 11/730 or 3200 computers.

(30) Collman, J. P.; Brauman, J. I.; Doxsee, K. M.; Halbert, T. R.; Bunnenberg, E.; Linder, R. E.; La Mar, G. N.; Del Gaudio, J. D.; Lang, G.; Spartalian, K. *J. Am. Chem. Soc.* **1980**, *102*, 4182.

(31) Safo, M. K.; Scheidt, W. R.; Gupta, G. P. *Inorg. Chem.* **1990**, *29*, 626.

(32) Dolphin, D.; Sams, J. R.; Tsin, T. B.; Wong, K. L. *J. Am. Chem. Soc.* **1976**, *98*, 6970.

(33) Epstein, L. M.; Straub, D. K.; Maricondi, C. *Inorg. Chem.* **1967**, *6*, 1720.

(34) Medhi, O. K.; Silver, J. *Inorg. Chim. Acta* **1989**, *166*, 129.

(35) Münck, E. *Methods Enzymol.* **1978**, *54*, 346.

(36) Straub, D. K.; Connor, W. M. *Ann. N.Y. Acad. Sci.* **1973**, *206*, 383.

Table 2. Mössbauer Data for Bis(imidazole and pyridine) Iron(II) Porphyrinates

complex	medium[a]	*T*, K (appl field)	δ,[b] mm s^{-1}	ΔE_Q, mm s^{-1}	lw, mm s^{-1}	ref
[Fe(TMP)(1-MeIm)$_2$]	crystalline	120	0.43(1)	1.11(1)	0.33(1)	this work
		4.2	0.45(1)	1.09(1)	0.30(1)	
[Fe(TMP)(4-NMe$_2$Py)$_2$]	crystalline	120	0.36(1)	1.27(1)	0.38(1)	this work
		4.2	0.39(1)	1.20(1)	0.27(1)	
[Fe(TMP)(4-CNPy)$_2$]	crystalline	120	0.41(1)	1.13(1)	0.27(2)	this work
		4.2	0.42(1)	1.11(1)	0.24(2)	
[Fe(TMP)(4-MePy)$_2$]	crystalline	120	0.42(1)	1.12(1)	0.27(1)	this work
		4.2	0.43(1)	1.09(1)	0.26(1)	
[Fe(TMP)(Py)$_2$]	crystalline	120	0.45(5)	1.24(5)	0.41(7)	this work
		4.2	0.46(2)	1.24(2)	0.32(3)	
[Fe(TMP)(3-ClPy)$_2$]	crystalline	120	0.43(2)	1.23(2)	0.31(3)	this work
		4.2	0.45(1)	1.24(1)	0.29(1)	
[Fe(TMP)(1-VinIm)$_2$]	crystalline	77	0.45	1.01	0.23	31
		4.2	0.43	1.00	0.26	
[Fe(TPP)(1-VinIm)$_2$]	crystalline	77	0.45	1.02	0.23	31
		4.2	0.43	1.00	0.26	
		4.2 (6 T)	0.46	1.02	0.23	
[Fe(TPP)(1-SiMe$_3$Im)$_2$]	crystalline	77	0.46	1.04	0.23	31
		4.2	0.46	1.03	0.23	
		4.2 (6 T)	0.46	1.03	0.23	
[Fe(TPP)(1-BzlIm)$_2$]	crystalline	77	0.45	1.02	0.23	31
[Fe(TPP)(1-AcIm)$_2$]	crystalline	77	0.45	0.97	0.22	31
[Fe(TPP)(1-MeIm)$_2$]	crystalline	77	0.47	1.07	0.25	31
[Fe(Proto IX)(1-MeIm)$_2$]	frozen EtOH:H$_2$O	78	0.47	1.03	0.15	34
[Fe(Proto IX)(HIm)$_2$]	frozen EtOH:H$_2$O	150	0.45	0.97	0.14	34
cytochrome b$_5$, reduced	frozen H$_2$O		0.43	1.04		34
[Fe(PClPP)(Py)$_2$]	crystalline	298	0.36	1.27		33
[Fe(OEP)(Py)$_2$]	crystalline	295	0.38	1.21		32
		4.2	0.46	1.13		
[Fe(Proto IX)(Py)$_2$]	crystalline	77	0.45	1.21		32
[Fe(TPP)(Py)$_2$]	crystalline	300	0.35	1.22		38
		77	0.40	1.15		
[Fe(TMP)(2-MeHIm)$_2$]	frozen DMA[c]	77	0.39	1.64		39
[Fe(TMP)(2-MeHIm)$_2$]		4.2 (6 T)	0.39	1.61	0.36	40
[Fe(TMP)(1,2-Me$_2$Im)$_2$]	frozen DMA[c]	77	0.39	1.73		39
[Fe(OEP)(2-MeHIm)$_2$]	frozen DMA[c]	77	0.34	1.67		39

[a] Crystalline samples contain natural abundance ^{57}Fe; frozen solution samples contain enriched ^{57}Fe. [b] All values relative to metallic iron. [c] DMA = dimethylacetamide.

of low-spin Fe(II) porphyrinates having electronegative donor atoms,[32−41] and the isomer shifts and quadrupole splittings lie within very narrow ranges (0.36−0.47 and 1.00−1.27 mm/s, respectively). Since only small sample quantities were available and spectral absorptions were correspondingly small, magnetic Mössbauer measurements were not feasible. The sign and symmetry of the EFG at the iron therefore remains unknown for the complexes of this study, but we recall that in all bis-ligated low-spin Fe(II) porphyrinates studied so far an excess of negative charge has been found in the porphyrin plane relative to the normal, suggesting a larger population in the d_{xy} orbital than in the d_π orbitals, perhaps as a result of charge transfer to the ligands.[42] In support of this expectation, the magnetic Mössbauer spectra of [Fe(TMP)(1-MeIm)$_2$], [Fe(TMP)(2-MeHIm)$_2$], and [Fe(OEP)(PMe$_3$)$_2$] reported elsewhere[40] show that V_{zz} is positive in all three of these complexes, and that there is a slight excess population in the d_{xy} orbital as compared to the d_π orbitals. However, on balance, the work summarized below indicates that there is little π back-bonding from the d_π orbitals to the axial ligands.

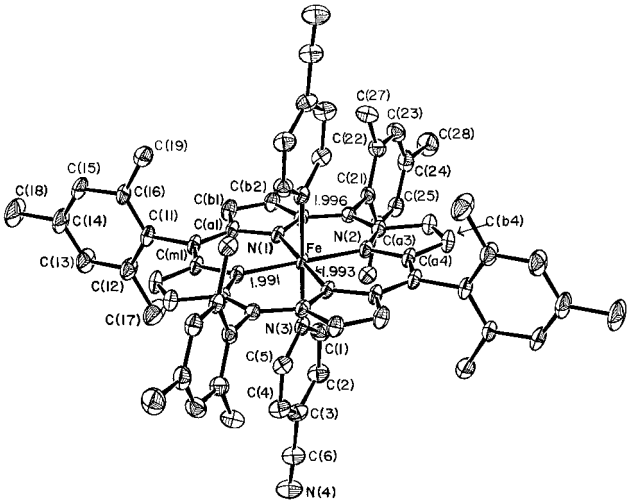

Figure 1. ORTEP diagram of [Fe(TMP)(4-CNPy)$_2$]. Labels assigned to the crystallographically unique molecule are displayed and 50% probability surfaces are shown.

Structures of the Complexes. The molecular structures of three of the seven complexes, [Fe(TMP)(4-CNPy)$_2$], [Fe(TMP)-(3-CNPy)$_2$], and [Fe(TMP)(4-MePy)$_2$], have been determined. Shown in ORTEP diagrams in Figures 1−3 are the molecular structures of these three complexes, respectively. The numbering scheme for the crystallographically unique atoms and bond distances in each coordination group are displayed in these

(37) Bearden, A. J.; Moss, T. H.; Caughey, W. S.; Beaudreau, C. A. *Proc. Natl. Acad. Sci. U.S.A.* **1965**, *53*, 1246. Bearden, A. J.; Moss, T. H.; Caughey, W. S.; Beaudreau, C. A. *Inorg. Chem.* **1966**, *5*, 1255.
(38) Kobayashi, H.; Maeda, Y.; Yanagawa, Y. *Bull. Chem. Soc. Jpn.* **1970**, *43*, 2342.
(39) Polam, J. R.; Wright, J. L.; Christensen, K. A.; Walker, F. A.; Flint, H.; Winkler, H.; Grodzicki, M.; Trautwein, A. X. *J. Am. Chem. Soc.* **1966**, *118*, 5272.
(40) Grodzicki, M.; Flint, H.; Winkler, H.; Walker, F. A.; Trautwein, A. X. *J. Phys. Chem. A* **1997**, *101*, 4202.
(41) Abu-Soud, H. M.; Silver, J. *Inorg. Chim. Acta* **1989**, *161*, 139.
(42) Debrunner, P. G. In *Iron Porphyrins*; Lever, A. B. P., Gray, H. B., Eds.; VCH Publishers: New York, 1989; Vol. 3, p 170.

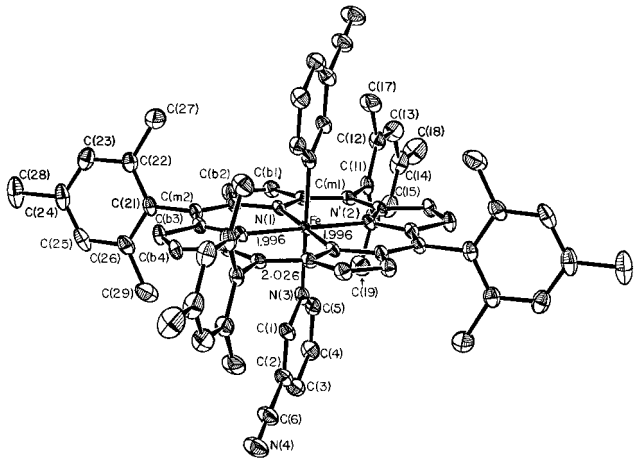

Figure 2. ORTEP diagram of [Fe(TMP)(3-CNPy)$_2$]. Labels assigned to the crystallographically unique molecule are displayed and 50% probability surfaces are shown.

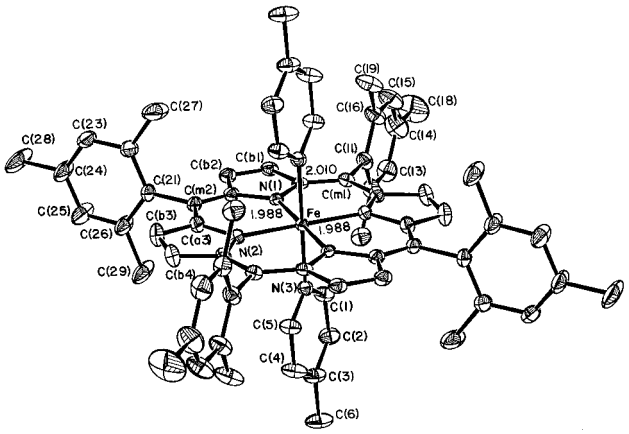

Figure 3. ORTEP diagram of [Fe(TMP)(4-MePy)$_2$]. Labels assigned to the crystallographically unique molecule are displayed and 50% probability surfaces are shown.

figures. All three complexes have crystallographically required inversion centers at the iron(II) atoms. This symmetry element leads to several requirements for the molecular structure. First, the iron(II) atom must be centered in the mean plane of the 24-atom core. Second, the axial ligand planes must be parallel to each other, and third, the porphinato cores cannot be significantly nonplanar. Previously reported molecular structures of three bis-imidazole iron(II) porphyrinates, [Fe(TPP)(1-VinIm)$_2$],[31] [Fe(TPP)(1-BzylIm)$_2$],[31] and [Fe(TPP)(1-MeIm)$_2$],[43] and two bis-pyridine complexes, [Fe(TPP)(Py)$_2$]·2Py[44] and [Fe(TPP)(Py)$_2$],[45] also have crystallographically required inversion symmetry and hence all conditions also apply to these molecules.

Averaged values for the chemically equivalent bond distances and angles for the three complexes of this study are shown in Figures 4−6. The number in parentheses following each averaged value is the estimated standard deviation calculated on the assumption that the individual values are all drawn from the same population. Individual values of the Fe−N$_P$ bond distances and their relationship to the axial ligand orientations are also shown in the diagrams. Fixed atomic coordinates for [Fe(TMP)(4-CNPy)$_2$], [Fe(TMP)(3-CNPy)$_2$], and [Fe(TMP)(4-MePy)$_2$] are given in Tables S2−S4, respectively, in the Supporting Information. Complete individual values of bond distances and angles for [Fe(TMP)(4-CNPy)$_2$], [Fe(TMP)(3-CNPy)$_2$], and [Fe(TMP)(4-MePy)$_2$] are given in Tables 3−8, respectively. Equatorial bond distances (Fe−N$_P$) average to

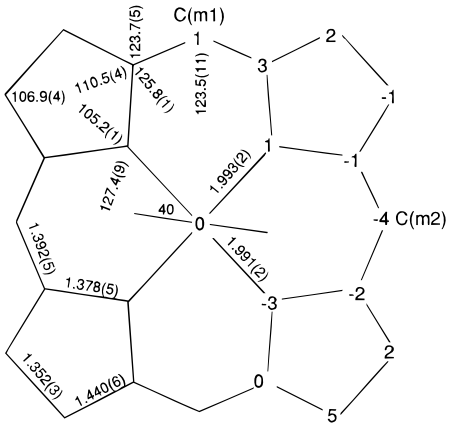

Figure 4. Formal diagram of the porphinato core in [Fe(TMP)(4-CNPy)$_2$]. Deviations of each unique atom from the mean plane of the core (in units of 0.01 Å) are shown. Averaged values for the chemically unique bond distances and angles in the core are shown. The orientation of the axial ligands with the closest Fe−N$_P$ vector (angle ϕ) are shown. Individual values of the Fe−N$_P$ bond distances are shown.

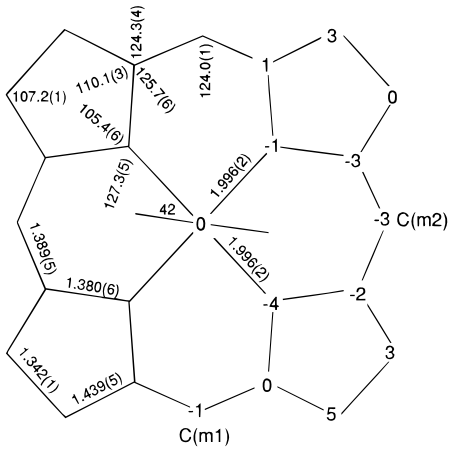

Figure 5. Formal diagram of the porphinato core in [Fe(TMP)(3-CNPy)$_2$]. Deviations of each unique atom from the mean plane of the core (in units of 0.01 Å) are shown. The same information displayed in Figure 4 is given.

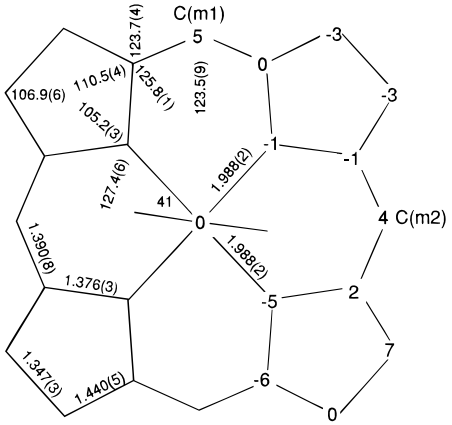

Figure 6. Formal diagram of the porphinato core in [Fe(TMP)(4-MePy)$_2$]. Deviations of each unique atom from the mean plane of the core (in units of 0.01 Å) are shown. The same information displayed in Figure 4 is given.

(43) (a) Steffen, W. L.; Chun, H. K.; Hoard, J. L.; Reed, C. A. *Abstracts of Papers*; 175th National Meeting of the American Chemical Society, Anaheim, CA; March 13, 1978; American Chemical Society: Washington, D.C., 1978; INOR 15. (b) Hoard, J. L., personal communication to W.R.S.

(44) Li, N.; Petricek, V.; Coppens, P.; Landrum, J. *Acta Crystallogr., Sect. C* **1985**, *C41*, 902.

(45) Li, N.; Coppens, P.; Landrum, J. *Inorg. Chem.* **1988**, *27*, 482.

Table 3. Bond Lengths in [Fe(TMP)(4-CNPy)$_2$]·2CHCl$_3$[a]

type	length, Å	type	length, Å
Fe−N(1)	1.993(2)	C(14)−C(15)	1.371(5)
Fe−N(2)	1.991(2)	C(14)−C(18)	1.508(5)
Fe−N(3)	1.996(2)	C(15)−C(16)	1.397(4)
N(1)−C(a1)	1.380(3)	C(16)−C(11)	1.399(4)
N(1)−C(a2)	1.370(4)	C(16)−C(19)	1.502(5)
N(2)−C(a3)	1.382(4)	C(21)−C(22)	1.401(4)
N(2)−C(a4)	1.379(3)	C(22)−C(23)	1.392(5)
N(3)−C(1)	1.354(4)	C(22)−C(27)	1.508(5)
N(3)−C(5)	1.350(4)	C(23)−C(24)	1.383(5)
C(a1)−C(b1)	1.443(4)	C(24)−C(25)	1.392(5)
C(a1)−C(m1)	1.387(4)	C(24)−C(28)	1.504(5)
C(a2)−C(b2)	1.441(4)	C(25)−C(26)	1.388(4)
C(a2)−C(m2)	1.400(4)	C(26)−C(21)	1.405(4)
C(a3)−C(b3)	1.444(4)	C(26)−C(29)	1.511(4)
C(a3)−C(m2)	1.391(4)	C(1)−C(2)	1.366(4)
C(a4)−C(b4)	1.431(4)	C(2)−C(3)	1.392(5)
C(a4)−C(m1)	1.390(4)	C(3)−C(4)	1.385(4)
C(b1)−C(b2)	1.354(4)	C(4)−C(5)	1.368(4)
C(b3)−C(b4)	1.350(4)	C(3)−C(6)	1.445(4)
C(m1)−C(11)	1.496(4)	C(6)−N(4)	1.143(4)
C(m2)−C(21)	1.491(4)	C(7)−Cl(1)	1.675(14)
C(11)−C(12)	1.394(4)	C(7)−Cl(2)	1.350(22)
C(12)−C(13)	1.393(4)	C(7)−Cl(3)	1.437(19)
C(12)−C(17)	1.515(5)	C(8)−Cl(4)	1.90(5)
C(13)−C(14)	1.379(5)	C(8)−Cl(5)	1.32(3)
C(8)−Cl(6)	1.42(3)		

[a] The estimated standard deviations of the least significant digits are given in parentheses. Primed and unprimed symbols denote a pair of atoms related by an inversion center at iron.

Table 4. Bond Angles in [Fe(TMP)(4-CNPy)$_2$]·2CHCl$_3$[a]

type	value, deg	type	value, deg
N(1)FeN(2)	89.16(9)	C(11)C(12)C(13)	119.3(3)
N(1)FeN(2)′	90.84(9)	C(11)C(12)C(17)	120.9(3)
N(1)FeN(3)	89.44(9)	C(13)C(12)C(17)	119.8(3)
N(2)FeN(3)	91.04(10)	C(12)C(13)C(14)	121.7(3)
FeN(1)C(a1)	126.56(20)	C(13)C(14)C(15)	118.4(3)
FeN(1)C(a2)	128.27(18)	C(13)C(14)C(18)	121.3(4)
C(a1)N(1)C(a2)	105.15(23)	C(15)C(14)C(18)	120.3(4)
FeN(2)C(a3)	128.07(18)	C(14)C(15)C(16)	122.2(3)
FeN(2)C(a4)	126.62(20)	C(11)C(16)C(15)	118.7(3)
C(a3)N(2)C(a4)	105.25(23)	C(11)C(16)C(19)	121.4(3)
FeN(3)C(1)	121.00(21)	C(15)C(16)C(19)	120.0(3)
FeN(3)C(5)	122.21(20)	C(m2)C(21)C(22)	120.2(3)
C(1)N(3)C(5)	116.7(3)	C(m2)C(21)C(26)	120.2(3)
N(1)C(a1)C(b1)	110.4(3)	C(22)C(21)C(26)	119.6(3)
C(b1)C(a1)C(m1)	123.8(3)	C(21)C(22)C(23)	119.0(3)
N(1)C(a1)C(m1)	125.8(3)	C(21)C(22)C(27)	120.6(3)
N(1)C(a2)C(b2)	111.02(24)	C(23)C(22)C(27)	120.4(3)
C(b2)C(a2)C(m2)	123.1(3)	C(22)C(23)C(24)	122.2(3)
N(1)C(a2)C(m2)	125.9(3)	C(23)C(24)C(25)	118.1(3)
N(2)C(a3)C(b3)	110.2(2)	C(23)C(24)C(28)	121.5(3)
C(b3)C(a3)C(m2)	124.0(3)	C(25)C(24)C(28)	120.3(3)
N(2)C(a3)C(m2)	125.8(3)	C(24)C(25)C(26)	121.5(3)
N(2)C(a4)C(b4)	110.4(3)	C(21)C(26)C(25)	119.6(3)
C(b4)C(a4)C(m1)′	123.8(3)	C(21)C(26)C(29)	120.7(3)
N(2)C(a4)C(m1)	125.8(3)	C(25)C(26)C(29)	119.9(3)
C(a1)C(b1)C(b2)	107.0(3)	N(3)C(1)C(2)	123.6(3)
C(a2)C(b2)C(b1)	106.5(3)	C(1)C(2)C(3)	118.5(3)
C(a3)C(b3)C(b4)	106.6(3)	C(2)C(3)C(4)	118.8(3)
C(a4)C(b4)C(b3)	107.5(3)	C(3)C(4)C(5)	119.0(3)
C(a1)C(m1)C(a4)′	124.3(3)	C(4)C(5)N(3)	123.3(3)
C(a1)C(m1)C(11)	118.0(3)	C(2)C(3)C(6)	120.2(3)
C(a4)'C(m1)C(11)	117.6(3)	C(4)C(3)C(6)	120.9(3)
C(a2)C(m2)C(a3)	122.7(3)	C(3)C(6)N(4)	178.2(4)
C(a2)C(m2)C(21)	118.9(3)	Cl(1)C(7)Cl(2)	114.0(13)
C(a3)C(m2)C(21)	118.4(3)	Cl(1)C(7)Cl(3)	107.3(10)
C(m1)C(11)C(12)	120.4(3)	Cl(2)C(7)Cl(3)	114.6(18)
C(m1)C(11)C(16)	119.8(3)	Cl(4)C(8)Cl(5)	129(3)
C(12)C(11)C(16)	119.8(3)	Cl(4)C(8)Cl(6)	95.0(18)
		Cl(5)C(8)Cl(6)	125.8(3)

[a] The estimated standard deviations of the least significant digits are given in parentheses. Primed and unprimed symbols denote a pair of atoms related by an inversion center at iron.

1.992(1) Å in [Fe(TMP)(4-CNPy)$_2$], 1.996(0) Å in [Fe(TMP)-(3-CNPy)$_2$], and 1.988(0) Å in [Fe(TMP)(4-MePy)$_2$]. These compare with those of other iron(II) porphyrinates: 1.997(6) Å in [Fe(TPP)(1-VinIm)$_2$],[31] 1.993(9) Å in [Fe(TPP)(1-BzylIm)$_2$],[31] and 1.997(6) Å in [Fe(TPP)(1-MeIm)$_2$].[43] The distances in the two bis-pyridine complexes, [Fe(TPP)(Py)$_2$]·2Py[44] and [Fe(TPP)(Py)$_2$],[45] are 1.993(6) and 2.002(1) Å, respectively. A pyrazine complex in which the ligands have a dihedral angle to each other of 40°,[46] has Fe−N$_P$ = 2.004(3) Å, a bis-piperidine complex[47] has Fe−N$_P$ = 2.004(3) Å, and a bis-tetrahydrothiophene complex[48] has Fe−N$_P$ = 1.996(6) Å. The structure of a highly distorted halogenated iron(II) porphyrinate with axial pyridine ligands in nearly perpendicular planes, has recently been reported.[49]

Of the three complexes whose structures we report herein, the axial bond lengths exhibit no clear trend that would indicate strong $d_\pi-p_\pi$ back-bonding for low-basicity pyridines: The Fe−N$_{ax}$ bond distance is 1.996(2) Å in [Fe(TMP)(4-CNPy)$_2$], 2.026 Å in [Fe(TMP)(3-CNPy)$_2$], and 2.010 Å in [Fe(TMP)(4-MePy)$_2$], where the order given is that expected for increasing σ-donor, decreasing π-acceptor characteristics of the axial ligands. These distances are comparable to those of the bis-imidazole Fe^{II}TPP complexes (see Table 9 for values), but slightly shorter than the values found in the two bis-pyridine Fe^{II}TPP complexes reported by Coppens and co-workers.[44,45]

An informative comparison can be made with the series of low-spin bis-pyridine iron(III) TMP complexes, where the axial Fe−N$_{ax}$ bond distances are also considered. Values for these iron(III) complexes and the iron(II) complexes are given in Table 9. The axial bond distances of [Fe(TMP)(4-CNPy)$_2$], [Fe-(TMP)(3-CNPy)$_2$], and [Fe(TMP)(4-MePy)$_2$] are longer than that found for the iron(III) TMP complex, [Fe(TMP)(4-NMe$_2$Py)$_2$]-ClO$_4$ (1.984(8) Å).[21] However, the distances are comparable to those of the other three Fe(III) complexes, [Fe(TMP)(3-EtPy)$_2$]ClO$_4$ (1.996(9) Å),[22] [Fe(TMP)(4-CNPy)$_2$]ClO$_4$ (2.011-(14) Å),[22] and [Fe(TMP)(3-ClPy)$_2$]ClO$_4$ (2.012(8) Å).[22] Slightly lengthened Fe−N$_{ax}$ bonds are found among imidazole complexes of Fe(II)[31] as compared to Fe(III),[50−53] Table 9.

For the three reported bis-pyridine Fe^{II}TMP complexes, the dihedral angles between the pyridine planes and the porphyrin cores show some modest deviations; the angles are 84.4°, 86.5°, and 84.0° in [Fe(TMP)(4-CNPy)$_2$], [Fe(TMP)(3-CNPy)$_2$], and [Fe(TMP)(4-MePy)$_2$], respectively. The dihedral angles between the porphyrin core and the mesityl groups are 88.6° and 85.7° in [Fe(TMP)(4-CNPy)$_2$], 80.7° and 88.5° in [Fe(TMP)-(3-CNPy)$_2$], and 86.9° and 87.8° in [Fe(TMP)(4-MePy)$_2$].

A sterically bulky porphyrin and pyridine ligands were successfully used to control axial ligand orientation in the low-spin Fe^{III}TMP systems.[21,22] We naively expected that the

(46) Hiller, W.; Hanack, M.; Mezger, M. G. *Acta Crystallogr., Sect. C* **1987**, *C43*, 1264.
(47) Radonovich, L. J.; Bloom, A.; Hoard, J. L. *J. Am. Chem. Soc.* **1972**, *94*, 2074.
(48) Mashiko, T.; Reed, C. A.; Haller, K. J.; Kastner, M. E.; Scheidt, W. R. *J. Am. Chem. Soc.* **1981**, *103*, 5758.
(49) Grinstaff, M. W.; Hill, M. G.; Birnbaum, R.; Schaefer, W. P.; Labinger, J. A.; Gray, H. B. *Inorg. Chem.* **1995**, *34*, 4896.
(50) Quinn, R.; Valentine, J. S.; Byrn, M. P.; Strouse, C. E. *J. Am. Chem. Soc.* **1987**, *109*, 3301.
(51) Scheidt, W. R.; Osvath, S. R.; Lee, Y. J. *J. Am. Chem. Soc.* **1987**, *109*, 1958.
(52) Collins, D. M.; Countryman, R.; Hoard, J. L. *J. Am. Chem. Soc.* **1972**, *94*, 2066.
(53) Little, R. G.; Dymock, K. R.; Ibers, J. A. *J. Am. Chem. Soc.* **1975**, *97*, 4532.

Table 5. Bond Lengths in [Fe(TMP)(3-CNPy)$_2$]·2CHCl$_3$[a]

type	length, Å	type	length, Å
Fe−N(1)	1.996(2)	C(14)−C(15)	1.395(5)
Fe−N(2)	1.996(2)	C(14)−C(18)	1.506(4)
Fe−N(3)	2.026(2)	C(15)−C(16)	1.394(4)
N(1)−C(a1)	1.386(3)	C(16)−C(11)	1.392(4)
N(1)−C(a2)	1.377(3)	C(16)−C(19)	1.505(4)
N(2)−C(a3)	1.374(3)	C(21)−C(22)	1.398(4)
N(2)−C(a4)	1.383(3)	C(22)−C(23)	1.388(4)
N(3)−C(1)	1.355(3)	C(22)−C(27)	1.506(5)
N(3)−C(5)	1.357(4)	C(23)−C(24)	1.379(5)
C(a1)−C(b1)	1.433(4)	C(24)−C(25)	1.380(5)
C(a1)−C(m1)	1.391(4)	C(24)−C(28)	1.510(4)
C(a2)−C(b2)	1.437(4)	C(25)−C(26)	1.394(4)
C(a2)−C(m2)	1.394(4)	C(26)−C(21)	1.402(4)
C(a3)−C(b3)	1.445(4)	C(26)−C(29)	1.498(4)
C(a3)−C(m2)	1.384(4)	C(1)−C(2)	1.384(4)
C(a4)−C(b4)	1.442(4)	C(2)−C(3)	1.388(4)
C(a4)−C(m1)′	1.385(4)	C(3)−C(4)	1.384(4)
C(b1)−C(b2)	1.343(4)	C(4)−C(5)	1.369(4)
C(b3)−C(b4)	1.341(4)	C(2)−C(6)	1.441(4)
C(m1)−C(11)	1.505(4)	C(6)−N(4)	1.141(4)
C(m2)−C(21)	1.498(4)	C(7)−Cl(1)	1.735(4)
C(11)−C(12)	1.398(4)	C(7)−Cl(2)	1.734(5)
C(12)−C(13)	1.399(4)	C(7)−Cl(3)	1.758(5)
C(12)−C(17)	1.493(4)	C(7)−Cl(4)	2.01(4)
C(13)−C(14)	1.370(5)	C(7)−Cl(5)	1.82(3)
		C(7)−Cl(6)	1.77(3)

[a] The estimated standard deviations of the least significant digits are given in parentheses. Primed and unprimed symbols denote a pair of atoms related by an inversion center at iron.

Table 6. Bond Angles in [Fe(TMP)(3-CNPy)$_2$]·2CHCl$_3$[a]

type	value, deg	type	value, deg
N(1)FeN(2)	90.31(9)	C(11)C(12)C(13)	118.3(3)
N(1)FeN(2)′	89.68(9)	C(11)C(12)C(17)	121.4(3)
N(1)FeN(3)	89.43(9)	C(13)C(12)C(17)	120.3(3)
N(2)FeN(3)	89.63(9)	C(12)C(13)C(14)	122.9(3)
FeN(1)C(a1)	127.83(18)	C(13)C(14)C(15)	117.8(3)
FeN(1)C(a2)	127.08(17)	C(13)C(14)C(18)	121.3(3)
C(a1)N(1)C(a2)	104.95(21)	C(15)C(14)C(18)	120.9(3)
FeN(2)C(a3)	126.74(17)	C(14)C(15)C(16)	121.4(3)
FeN(2)C(a4)	127.41(18)	C(11)C(16)C(15)	119.5(3)
C(a3)N(2)C(a4)	105.84(21)	C(11)C(16)C(19)	120.7(3)
FeN(3)C(1)	122.04(19)	C(15)C(16)C(19)	119.8(3)
FeN(3)C(5)	121.09(18)	C(m2)C(21)C(22)	120.85(24)
C(1)N(3)C(5)	116.86(24)	C(m2)C(21)C(26)	119.49(25)
N(1)C(a1)C(b1)	110.27(22)	C(22)C(21)C(26)	119.66(25)
C(b1)C(a1)C(m1)	124.73(24)	C(21)C(22)C(23)	119.5(3)
N(1)C(a1)C(m1)	125.00(24)	C(21)C(22)C(27)	120.8(3)
N(1)C(a2)C(b2)	110.37(22)	C(23)C(22)C(27)	119.6(3)
C(b2)C(a2)C(m2)	124.09(24)	C(22)C(23)C(24)	121.7(3)
N(1)C(a2)C(m2)	125.53(24)	C(23)C(24)C(25)	118.4(3)
N(2)C(a3)C(b3)	109.79(23)	C(23)C(24)C(28)	120.7(3)
C(b3)C(a3)C(m2)	123.86(25)	C(25)C(24)C(28)	120.9(3)
N(2)C(a3)C(m2)	126.33(24)	C(24)C(25)C(26)	122.1(3)
N(2)C(a4)C(b4)	109.78(23)	C(21)C(26)C(25)	118.7(3)
C(b4)C(a4)C(m1)′	124.39(24)	C(21)C(26)C(29)	121.0(3)
N(2)C(a4)C(m1)	125.83(23)	C(25)C(26)C(29)	120.3(3)
C(a1)C(b1)C(b2)	107.18(23)	N(3)C(1)C(2)	121.9(3)
C(a2)C(b2)C(b1)	107.22(24)	C(1)C(2)C(3)	120.8(3)
C(a3)C(b3)C(b4)	107.40(24)	C(2)C(3)C(4)	116.9(3)
C(a4)C(b4)C(b3)	107.18(23)	C(3)C(4)C(5)	120.2(3)
C(a1)C(m1)C(a4)′	124.13(24)	C(4)C(5)N(3)	123.4(3)
C(a1)C(m1)C(11)	117.69(23)	C(1)C(2)C(6)	119.4(3)
C(a4)′C(m1)C(11)	118.17(22)	C(3)C(2)C(6)	119.8(3)
C(a2)C(m2)C(a3)	123.94(25)	C(2)C(6)N(4)	178.7(4)
C(a2)C(m2)C(21)	118.03(22)	Cl(1)C(7)Cl(2)	110.5(3)
C(a3)C(m2)C(21)	117.99(23)	Cl(1)C(7)Cl(3)	110.06(23)
C(m1)C(11)C(12)	119.62(25)	Cl(2)C(7)Cl(3)	111.44(25)
C(m1)C(11)C(16)	120.23(24)	Cl(4)C(7)Cl(5)	93.9(14)
C(12)C(11)C(16)	120.15(25)	Cl(4)C(7)Cl(6)	141.9(15)
		Cl(5)C(7)Cl(6)	85.9(13)

[a] The estimated standard deviations of the least significant digits are given in parentheses. Primed and unprimed symbols denote a pair of atoms related by an inversion center at iron.

corresponding low-spin iron(II) complexes would show the same preferences for relative parallel or perpendicular orientations of the ligand planes. However, the crystal structures of the three bis-pyridine TMP complexes reported herein show the two axial ligands to be parallel to each other. The ligand planes make dihedral angles ϕ of 40°, 42°, and 41° to the closest Fe−N$_P$ axis in [Fe(TMP)(4-CNPy)$_2$], [Fe(TMP)(3-CNPy)$_2$], and [Fe(TMP)(4-MePy)$_2$], respectively. The dihedral angles of the two bis-pyridine iron(II) TPP complexes reported previously are also large, 34° and 43°.[44,45] Such large values are common for bis-pyridine complexes of both low-spin iron(II) and -(III).[21,31,44,45,54−56] In iron porphyrinate derivatives with planar cores, placing the pyridine rings above the Fe−N$_P$ bonds is always associated with longer axial bond lengths and hence the intermediate-spin state.[56−58] Because small dihedral angles are observed for many bis-imidazole complexes of iron(II) and -(III) porphyrinates,[21,31,43,50−53] and all such complexes are strictly low-spin, we conclude that the difference in "cone angle" as measured by interference between the "*ortho*"-H of the imidazole or pyridine rings and the electron density of the Fe−N$_P$ bonds is significant enough to allow 5-membered-ring heterocycles to have small dihedral angles while precluding such angles for 6-membered-ring heterocycles. Molecular mechanics (MM2) calculations confirm that the lowest-energy position for pyridine ligands is that with dihedral angles of 45°.[55]

In the three Fe^{II}TMP complexes the closest nonbonded distance between pyridine ligand atoms and the *o*-methyl carbon of the mesityl group is 3.80 Å in [Fe(TMP)(4-MePy)$_2$], 3.76 Å in [Fe(TMP)(4-CNPy)$_2$], and 3.72 Å in [Fe(TMP)(3-CNPy)$_2$]. It appears that none of these distances are short enough to cause serious nonbonded contacts. In the Fe(III) TMP analogs,[21,22] the porphinato core is S$_4$ ruffled with the mesityl rings concomitantly tipped away from the pyridines. This leads to much larger mesityl carbon−pyridine carbon distances which range from 3.8 Å upwards, with almost all greater than 4.2 Å. The depths of the ligand binding pockets (as measured by the *o*-methyl substituents of opposite mesityl rings) from the mean porphinato plane in each complex of the present study are similar, 2.52 and 2.52 Å in [Fe(TMP)(4-CNPy)$_2$], 2.48 and 2.50 Å in [Fe(TMP)(3-CNPy)$_2$], and 2.62 and 2.41 Å in [Fe(TMP)-(4-MePy)$_2$]. The square shape and symmetric depth contrast with the iron(III) TMP complexes, which have oblong pockets of unequal depth.[21,22]

The phenomenon of ruffling among all iron(III) complexes with perpendicular axial ligand orientations[21−23,55,59,60] has been explained in terms of steric interactions between the porphyrinate ring and its substituents and the axial ligands for the five Fe^{III}-TMP complexes reported by us[21−23] and also for [Fe(TPP)(2-MeHIm)$_2$]ClO$_4$.[60] However, these steric interactions cannot explain the perpendicular axial ligand orientations and ruffled

(54) Inniss, D.; Soltis, S. M.; Strouse, C. E. *J. Am. Chem. Soc.* **1988**, *110*, 5644.
(55) Safo, M. K.; Walker, F. A.; Raitsimring, A. M.; Walters, W. P.; Dolata, D. P.; Debrunner, P. G.; Scheidt, W. R. *J. Am. Chem. Soc.* **1994**, *116*, 7760.
(56) Scheidt, W. R.; Geiger, D. K.; Haller, K. J. *J. Am. Chem. Soc.* **1982**, *104*, 495.
(57) Safo, M. K.; Scheidt, W. R.; Gupta, G. P.; Orosz, R. D.; Reed, C. A. *Inorg. Chim. Acta* **1991**, *184*, 251.
(58) Scheidt, W. R.; Geiger, D. K.; Hayes, R. G.; Lang, G. *J. Am. Chem. Soc.* **1983**, *105*, 2625.
(59) Hatano, K.; Safo, M. K.; Walker, F. A.; Scheidt, W. R. *Inorg. Chem.* **1991**, *30*, 1643.
(60) Scheidt, W. R.; Kirner, J. L.; Hoard, J. L.; Reed, C. A. *J. Am. Chem. Soc.* **1987**, *109*, 1963.

Table 7. Bond Lengths in $[Fe(TMP)(4\text{-}MePy)_2]\cdot 2C_6H_6$[a]

type	length, Å	type	length, Å
Fe−N(1)	1.988(2)	C(16)−C(11)	1.398(4)
Fe−N(2)	1.988(2)	C(16)−C(19)	1.502(4)
Fe−N(3)	2.010(2)	C(21)−C(22)	1.394(4)
N(1)−C(a1)	1.379(3)	C(22)−C(23)	1.392(5)
N(1)−C(a2)	1.378(3)	C(22)−C(27)	1.495(4)
N(2)−C(a3)	1.372(3)	C(23)−C(24)	1.367(4)
N(2)−C(a4)	1.374(3)	C(24)−C(25)	1.385(4)
N(3)−C(1)	1.341(3)	C(24)−C(28)	1.510(4)
N(3)−C(5)	1.338(3)	C(25)−C(26)	1.384(4)
C(a1)−C(b1)	1.440(3)	C(26)−C(21)	1.393(4)
C(a1)−C(m1)	1.392(3)	C(26)−C(29)	1.507(4)
C(a2)−C(b2)	1.439(3)	C(1)−C(2)	1.376(3)
C(a2)−C(m2)	1.377(3)	C(2)−C(3)	1.384(4)
C(a3)−C(b3)	1.434(3)	C(3)−C(4)	1.384(4)
C(a3)−C(m2)	1.394(3)	C(4)−C(5)	1.379(3)
C(a4)−C(b4)	1.446(3)	C(3)−C(6)	1.499(3)
C(a4)−C(m1)′	1.395(3)	C(30)−C(31)	1.344(18)
C(b1)−C(b2)	1.345(4)	C(31)−C(32)	1.302(20)
C(b3)−C(b4)	1.349(4)	C(32)−C(33)	1.334(21)
C(m1)−C(11)	1.502(3)	C(33)−C(34)	1.487(20)
C(m2)−C(21)	1.502(3)	C(34)−C(35)	1.71(14)
C(11)−C(12)	1.396(4)	C(35)−C(31)	1.306(14)
C(12)−C(13)	1.386(4)	C(36)−C(37)	1.303(22)
C(12)−C(17)	1.504(4)	C(37)−C(38)	1.20(4)
C(13)−C(14)	1.399(4)	C(38)−C(39)	1.51(3)
C(14)−C(15)	1.372(5)	C(36)−C(37)	1.53(3)
C(14)−C(18)	1.511(5)	C(36)−C(37)	1.48(3)
C(15)−C(16)	1.389(4)	C(36)−C(37)	1.415(20)

[a] The estimated standard deviations of the least significant digits are given in parentheses. Primed and unprimed symbols denote a pair of atoms related by an inversion center at iron.

Table 8. Bond Angles in $[Fe(TMP)(4\text{-}MePy)_2]\cdot C_6H_6$[a]

type	value, deg	type	value, deg
N(1)FeN(2)	90.47(8)	C(12)C(13)C(14)	121.3(3)
N(1)FeN(2)′	89.53(7)	C(13)C(14)C(15)	118.1(3)
N(1)FeN(3)	90.80(7)	C(13)C(14)C(18)	120.5(4)
N(2)FeN(3)	91.55(7)	C(15)C(14)C(18)	121.4(4)
FeN(1)C(a1)	127.74(15)	C(14)C(15)C(16)	122.4(3)
FeN(1)C(a2)	126.85(16)	C(11)C(16)C(15)	118.2(3)
C(a1)N(1)C(a2)	105.40(19)	C(11)C(16)C(19)	121.1(3)
FeN(2)C(a3)	126.86(16)	C(15)C(16)C(19)	120.1(3)
FeN(2)C(a4)	128.05(15)	C(m2)C(21)C(22)	120.17(21)
C(a3)N(2)C(a4)	104.93(19)	C(m2)C(21)C(26)	120.14(22)
FeN(3)C(1)	121.61(16)	C(22)C(21)C(26)	119.69(23)
FeN(3)C(5)	122.35(16)	C(21)C(22)C(23)	119.36(23)
C(1)N(3)C(5)	115.98(20)	C(21)C(22)C(27)	120.65(23)
N(1)C(a1)C(b1)	110.18(20)	C(23)C(22)C(27)	119.98(24)
C(b1)C(a1)C(m1)	123.85(22)	C(22)C(23)C(24)	121.87(24)
N(1)C(a1)C(m1)	125.96(21)	C(23)C(24)C(25)	117.8(3)
N(1)C(a2)C(b2)	111.13(21)	C(23)C(24)C(28)	121.9(3)
C(b2)C(a2)C(m2)	124.02(22)	C(25)C(24)C(28)	120.3(3)
N(1)C(a2)C(m2)	125.82(22)	C(24)C(25)C(26)	122.5(3)
N(2)C(a3)C(b3)	110.72(22)	C(21)C(26)C(25)	118.74(24)
C(b3)C(a3)C(m2)	123.67(23)	C(21)C(26)C(29)	121.17(24)
N(2)C(a3)C(m2)	125.60(22)	C(25)C(26)C(29)	120.09(24)
N(2)C(a4)C(b4)	110.88(20)	N(3)C(1)C(2)	123.81(22)
C(b4)C(a4)C(m1)′	123.20(22)	C(1)C(2)C(3)	120.08(24)
N(2)C(a4)C(m1)	125.82(21)	C(2)C(3)C(4)	116.29(22)
C(a1)C(b1)C(b2)	107.03(21)	C(3)C(4)C(5)	120.30(24)
C(a2)C(b2)C(b1)	107.24(21)	C(4)C(5)N(3)	123.52(23)
C(a3)C(b3)C(b4)	107.37(22)	C(2)C(3)C(6)	120.79(24)
C(a4)C(b4)C(b3)	106.06(22)	C(4)C(3)C(6)	122.89(25)
C(a1)C(m1)C(a4)′	122.87(22)	C(31)C(30)C(35)	116.3(13)
C(a1)C(m1)C(11)	118.53(21)	C(30)C(31)C(32)	120.5(15)
C(a4)′C(m1)C(11)	118.59(21)	C(31)C(32)C(33)	127.0(14)
C(a2)C(m2)C(a3)	124.13(22)	C(32)C(33)C(34)	113.5(11)
C(a2)C(m2)C(21)	118.35(21)	C(33)C(34)C(35)	114.6(10)
C(a3)C(m2)C(21)	117.52(22)	C(34)C(35)C(36)	127.0(11)
C(m1)C(11)C(12)	120.18(22)	C(37)C(36)C(41)	118.1(15)
C(m1)C(11)C(16)	119.82(23)	C(36)C(37)C(38)	133.4(15)
C(12)C(11)C(16)	120.00(24)	C(37)C(38)C(39)	119.3(24)
C(11)C(12)C(13)	119.39(25)	C(38)C(39)C(40)	113.4(20)
C(11)C(12)C(17)	120.91(23)	C(39)C(40)C(41)	117.5(14)
C(13)C(12)C(17)	119.69(24)	C(40)C(41)C(36)	118.2(13)

[a] The estimated standard deviations of the least significant digits are given in parentheses. Primed and unprimed symbols denote a pair of atoms related by an inversion center at iron.

porphinato cores of $[Fe(TPP)(Py)_2]ClO_4$,[54] $[Fe(TPP)(4\text{-}CNPy)_2]ClO_4$,[55] and $[Fe((2,6\text{-}Cl_2)_4TPP)(1\text{-}VinIm)_2]ClO_4$.[59] For $[Fe(TPP)(4\text{-}CNPy)_2]ClO_4$ we have argued that there is an electronic reason for the ruffling;[55] the relatively strong π-acceptor (and weak σ-donor) properties of the 4-CNPy ligands stabilize the d_{xz},d_{yz} orbitals of low-spin Fe(III) to the point where their energy drops below that of the d_{xy} orbital, causing the latter to be the half-filled orbital. The filled d_{xz},d_{yz} set could thus be involved in π donation to the empty π^* orbitals of the pyridine ligands that have large wavefunction amplitude at the bonding nitrogen. Meanwhile, the half-filled d_{xy} orbital can then participate in strong porphyrin→Fe π donation from the filled $3a_{2u}(\pi)$ porphyrin orbital *if and only if* the porphyrinate ring ruffles significantly so as to twist the porphyrin nitrogen p_z orbitals by 15° or more from the normal to the mean plane of the porphyrin so that there is a significant p_z component in the *xy* plane,[55] and it is thus the porphyrin→Fe(III) π donation that stabilizes this ruffled complex. We have shown, based on MM2 calculations, that the energy involved in the core ruffling is relatively small in the iron(III) systems (4−8 kJ/mol).[55]

It is reasonable to expect that the porphyrin cores in the iron(II) TMP complexes will be ruffled if the axial ligands assume perpendicular orientation with the ligand planes aligned along the *meso* positions of the porphyrin because of a tendency of the porphyrinate ring to bend or fold away from the unopposed axial ligand (especially for pyridines or hindered imidazoles) along a line perpendicular to its plane. Such a tendency has been noted not only in the model ferriheme complexes discussed above but also in the structures of several cytochromes *c*,[61] where the histidine imidazole plane is aligned close to the α,γ *meso* positions, as well as for cytochrome *f*[12,62] and the siroheme of sulfite reductase.[63] A different and more obvious cause of ruffling arises if there are bulky substituents on both the *meso* and β-pyrrole positions of the porphyrin, as in the highly halogenated Fe(II) porphyrinate $[Fe(TFPPBr_8)(Py)_2]$,[49] where the porphyrinate ring *cannot* be planar and the axial ligands must follow the constraints of the ruffling pattern imposed by the bulky porphyrin. For the low-spin Fe(III) porphyrinates bound to ligands of moderate to high π-acceptor capability, we have pointed out, as mentioned in the previous paragraph, a third cause of ruffling that arises when the d_{xy} orbital contains the unpaired electron and can only receive electron density from the porphyrinate ring by π donation if the porphyrinate ring ruffles.[55,64] Because the d_{xy} orbital is filled in the case of low-spin d^6, this avenue for stabilizing perpendicular axial ligands is not available for the Fe(II) porphyrinates. The parallel ligand orientation, with the above-mentioned minimal contacts between the pyridine and mesityl carbons, thus becomes the thermodynamically stable form. Apparently, only with extremely bulky porphyrinate and ligand substituents, as in the bis(1,2-dimethylimidazole) complex of $Fe^{II}TMP$[8,26,39] discussed below, can perpendicular orientation of axial ligands be stabilized for an

(61) Hobbs, J. D.; Shelnutt, J. A. *J. Protein Chem.* **1995**, *14*, 19.
(62) Martinez, S. E.; Smith, J. L.; Huang, D.; Szczepaniak, A.; Cramer, W. A. In *Research in Photosynthesis*; Murata, N., Ed.; Proceedings of the IXth International Congress on Photosynthesis; Kluwer Academic: Dordrecht, The Netherlands, 1992; Vol. 2, p 495.
(63) Crane, B. R.; Sigel, L. M.; Getzoff, E. D. *Science* **1995**, *270*, 29.
(64) Walker, F. A.; Nasri, H.; Turowska-Tyrk, I.; Mohanrao, K.; Watson, C. T.; Shokhirev, N. V.; Debrunner, P. G.; Scheidt, W. R. *J. Am. Chem. Soc.* **1996**, *118*, 12109.

Table 9. Summary of Fe−N Bond Distances in Low-Spin Bis(imidazole and pyridine) Iron(II) and -(III) Complexes[a]

complex	Fe−N_p[b]	Fe−N_{ax}[b]	ref
A. Iron(II) Complexes			
[Fe(TPP)(1-VinIm)$_2$]	2.001(2)	2.004(2)	31
[Fe(TPP)(1-BzlIm)$_2$]	1.992(9)	2.017(4)	31
[Fe(TPP)(1-MeIm)$_2$]	1.997(6)	2.014(5)	43
[Fe(TMP)(4-CNPy)$_2$]	1.992(1)	1.996(2)	this work
[Fe(TMP)(4-MePy)$_2$]	1.988(0)	2.010(2)	this work
[Fe(TMP)(3-CNPy)$_2$]	1.996(0)	2.026(2)	this work
[Fe(TPP)(Py)$_2$]	2.001(2)	2.037(1)	45
[Fe(TPP)(Py)$_2$]·2Py	1.993(6)	2.039(1)	44
B. Iron(III) Complexes			
[Fe(TMP)(1-MeIm)$_2$]C1O$_4$[d]	1.988(20)	1.975(3)	21
	1.987(1)	1.965(3)	
[Fe(TPP)(HIm)$_2$]Cl·MeOH	1.989(8)	1.974(24)	52
[Fe(TPP)(HIm)$_2$]Cl·H_2O[d]	1.994(12)	1.977(3)	51
	1.993(4)	1.964(3)	
[Fe(Proto IX)(1-MeIm)$_2$]	1.991(16)	1.977(16)	53
[Fe(TPP)(2-MeHIm)$_2$]ClO$_4$	1.971(4)	2.013(4)	60
[Fe(TPP)(t-MU)$_2$]SbF_6	1.992(5)	1.983(4)	50
[Fe(TPP)(c-MU)$_2$]SbF_6[d]	1.997(1)	1.967(7)	50
	1.995(17)	1.979(7)	
[Fe(TMP)(4-NMe$_2$Py)$_2$]C1O$_4$	1.964(10)	1.984(8)	21
[Fe(TMP)(3-EtPy)$_2$]C1O$_4$	1.964(4)	1.996(9)	22
[Fe(TMP)(3-ClPy)$_2$]C1O$_4$	1.968(3)	2.012(8)	22
[Fe(TMP)(4-CNPy)$_2$]C1O$_4$	1.961(7)	2.011(14)	22
[Fe(TPP)(4-CNPy)$_2$]C1O$_4$	1.952(7)	2.002(8)	55
[Fe(OEP)(4-NMe$_2$Py)$_2$]C1O$_4$	2.002(4)	1.995(3)	21

[a] The numbers in parentheses are the estimated standard deviations in the least significant digit(s). [b] Values in angstroms. [c] Two independent half-molecules with required inversion symmetry.

Table 10. Fe^{III}/Fe^{II} Reduction Potentials and Equilibrium Constants for Binding Axial Ligands to Fe^{II}TMP in Dimethylformamide To Form [Fe(TMP)(L)$_2$][26]

ligand	pK_a(BH^+)[a]	Fe^{III}/Fe^{II} $E_{1/2}$, V[b]	log(β_2^{II})	log(β_2^{III})
4-CNPy	∼1.1	+0.331	7.5	0.2
Py	5.22	+0.140	7.4	3.3
3,4-Me$_2$Py	6.46	+0.077	7.3	4.4
4-NMe$_2$Py	9.7	−0.121	7.9	8.3
N-MeIm	7.33	−0.130	7.3	7.9
2-MeHIm	7.56	−0.212	5.5	7.4

[a] pK_a(BH^+) values taken from ref 65 except for that of 4-CNPy. See ref 22 for discussion of the basicity of the latter pyridine. [b] Potentials listed *vs* SCE. Measured in dimethylformamide at 25 °C; electrolyte = 0.03 M TBAP.

Fe(II) porphyrinate that does not have bulky substituents at *both* *meso* and β-pyrrole positions.

Equilibrium Constants for Formation of [Fe(TMP)L$_2$] Complexes. We have recently reported the complex stabilities and reduction potentials for a series of tetrakis(2,6-disubstituted phenyl)porphyrinatoiron(II)−bis-L complexes,[26] where L includes some of the same series of substituted pyridine and imidazole ligands as studied in this work. Among the so-called "hindered" porphyrinates studied were the tetramesitylporphyrinate complexes. Table 10 summarizes the Fe^{III}/Fe^{II} reduction potentials of the bis-ligated complexes and the equilibrium constants, log(β_2II), for binding the ligands to Fe^{II}TMP. Because the study was carried out in dimethylformamide solution, the complex formation reaction in each case is:

$$[Fe(TMP)(DMF)] + 2L \rightleftarrows [Fe(TMP)(L)_2] + DMF \quad (1)$$

$$\beta_2^{II} = [Fe(TMP)(L)_2]/[Fe(TMP)(DMF)][L]^2 \quad (2)$$

The remarkable finding for the TMP complexes (as well as for each of the other porphyrinates studied) is that the values of log(β_2^{II}) for the substituted pyridines studied are all within experimental error of each other,[26] even though the basicities of their conjugate acids, pK_a(PyH^+), range from ∼1.1 (4-CNPy) to 9.7 (4-NMe$_2$Py).[65] For each of the porphyrinates studied the same situation was found: log(β_2^{II}) is "leveled" to a particular value for each porphyrinate for the series of pyridines, indicating no sensitivity on the part of Fe(II) to the σ-donor or π-donor/acceptor characteristics of the axial ligands.[26] In contrast, the bis(1-MeIm) and bis(2-MeHIm) complexes of porphyrinates having large *ortho* substituents have similar values of log(β_2^{II}) (∼7.4 and ∼5.4, respectively), and do not appear to be sensitive to the nature of the substituents, while less "hindered" porphyrinate complexes do not form bis(2-MeHIm) complexes at ambient temperatures at ligand concentrations less than 1 M.[26]

While the values of log(β_2^{II}) are quite similar, the Fe^{III}/Fe^{II} reduction potentials of the [Fe(TMP)(L)$_2$] complexes listed in Table 10 vary strongly with the nature of the axial ligand. This is due to the fact that the equilibrium constants for binding the ligands to the Fe^{III}TMP complexes vary significantly with the basicity of the pyridine ligands and the steric factors of the imidazole ligands.[26] It should be noted that the Fe^{III}/Fe^{II} reduction potential is determined by the ratio of the equilibrium constants, log($\beta_2^{III}/\beta_2^{II}$), measured under high enough ligand concentration to ensure that the ratios of the concentrations of the bis complexes of both oxidation states are independent of ligand concentration.[26,66] Thus, the differences in reduction potentials, given the "leveled" values of β_2^{II}, are a measure of the values of β_2^{III}, and do not, *a priori*, give any information about bonding interactions in the Fe(II) (or Fe(III)) complexes.

Thus, the above-summarized work shows that only in the presence of very bulky substituents on the *ortho* positions of the phenyl rings of a (tetraphenylporphyrinato)iron(II) complex are the bis-ligand complexes of 2- or 1,2-alkyl-substituted imidazoles stable at room temperature at ligand concentrations less than 1 M,[26] and even for porphyrinates for which this complex can be formed (TMP, for example), the stabilities of the bis(2-MeHIm) complexes are approximately two orders of magnitude less than those of the corresponding bis(1-MeIm) and all bis(pyridine) complexes.[26] Although no structure of a bis(2-methylimidazole) or related complex of an Fe(II) porphyrinate has yet appeared, we have recently characterized the Fe(II) analog of this complex by 2D NMR techniques at very low temperatures (−70 to −90 °C), where axial ligand rotation is slow on the NMR time scale.[8] Our studies confirm that the axial 1,2-Me$_2$Im ligands are aligned in perpendicular planes, and the large difference in chemical shift of the two pairs of *o*-CH_3 mesityl resonances[8] is very strong evidence that the porphyrinate ring is strongly ruffled, as is observed in the Fe(III) analog, [Fe(TMP)(1,2-Me$_2$Im)$_2$]$^+$.[23] The Mössbauer isomer shifts and quadrupole splittings of [Fe(TMP)(2-MeHIm)$_2$], [Fe(OEP)(2-MeHIm)$_2$], and [Fe(TMP)(1,2-Me$_2$Im)$_2$] have recently been reported[39,40] (Table 2). The unusually large quadrupole splittings, ΔE_Q > 1.6 mm/s,[39,40] are unique for low-spin Fe(II) porphyrinates. Recent SCC-Xα calculations in the Local Density Approximation,[40] discussed below, indicate that the ruffling of the porphyrinate ring, which results in significant shortening of the Fe−N_P bonds, is the primary cause of the exceptionally large quadrupole splittings observed for the bis-(2-methyl- and -1,2-dimethylimidazole) complexes of Fe(II) porphyrinates (Table 2).

The necessity of utilizing more highly "hindered" axial ligands than the pyridines of this study (or highly congested porphyrins substituted at both *meso* and β-pyrrole positions[49])

(65) Albert, A. In *Physical Methods in Heterocyclic Chemistry*; Katritzky, A. R., Ed.; Academic Press: New York, 1971; Vol. I, pp 1−108, and Vol. III, pp 1−26. See also ref 22 for discussion of the pK_a(BH^+) of 4-CNPy.

(66) Kolthoff, I. M.; Lingane, J. J. *Polarography* **1952**, *1*, 221.

to force perpendicular orientation of unconstrained axial ligands in Fe(II) porphyrinate complexes raises the intriguing question of whether or not there may be an energetically unfavorable interaction, heretofore unrecognized, that makes perpendicular orientation of axial ligand planes unlikely in such unconstrained systems. Such an unfavorable energy term could result from the necessity for the porphyrinate ring to ruffle, and we have pointed out above and previously[23] that perpendicular orientation of planar axial ligands "encourages" the porphyrinate ring to ruffle. (We will explore the question of the energetics of ruffling in the final section of this paper.) In support of the hypothesis of an unfavorable energy term due to ruffling is the fact that one of the two histidine ligands of *Methylophilus methylotrophus* cytochrome *c″* is lost in a pH-dependent manner upon reduction of this protein from Fe(III) to Fe(II).[18b] Since the spectroscopic properties of ferric cytochrome *c″* strongly suggest that the axial histidine ligands are in perpendicular planes,[18] the loss of one histidine upon reduction is consistent with there being an unfavorable energy term involved in perpendicular orientation of planar axial ligands. (However, other effects, as yet unknown, imposed by the protein, may also contribute to this loss of histidine ligand upon reduction.)

As pointed out above, the Fe^{III}/Fe^{II} reduction potentials observed in these unconstrained model heme complexes are simply a measure of the relative stability of the Fe(III) and Fe(II) bis-ligand complexes, as measured by $\log(\beta_2^{III}/\beta_2^{II})$.[26,66] As we have seen (Table 10), forcing the ligands to be in perpendicular planes by choosing a "hindered" ligand such as 2-MeHIm reduces the value of β_2^{II} by a factor of nearly 100 over that for 1-MeIm, and this is the major contributor to the negative shift in the reduction potential of 82 mV (Table 10), for the values of β_2^{III} are very similar for the two ligands. Note that for unconstrained models, the perpendicularly-aligned axial ligand complex has the more *negative* (because of its lower stability) rather than the more positive reduction potential. We had predicted the potential of the perpendicularly-aligned ligand complex to be more positive previously,[19] and certainly the mitochondrial cytochromes *b*[17b,24] (presumed perpendicular imidazole planes) have more positive reduction potentials than do the cytochromes b_5[25] (known nearly parallel imidazole planes). Thus, it appears that while these unconstrained complexes are excellent spectroscopic and structural models of the bis-histidine cytochromes, they are not the best models for the effect of ligand orientation on reduction potential of the protein centers. They do not benefit from pre-organization of the heme binding site by hydrogen bonding of the histidine ligands in particular orientations. Also, hydrogen bonding of the histidine imidazole N−H itself can have profound effects upon complex stabilities[67] and thus reduction potentials. In this regard, it is interesting to note that in the presence of strong hydrogen-bond acceptors (triethylamine, for example), the "large g_{max}" signal of $[Fe(TPP)(2\text{-MeHIm})_2]^+$ is replaced by a "normal rhombic" signal,[68] suggesting that in the presence of stronger σ- and π-donation capabilities of the axial ligands the complex finds a way to place the bulky axial ligands in relative orientations that are closer to being parallel than perpendicular. Further spectroscopic and structural characterization of this complex is in progress.

***π* Donor/Acceptor Interactions in Low-Spin Fe(II) Porphyrinates.** The imidazole and high-basicity pyridine ligands of the Fe^{II}TMP derivatives of this study are all expected to form strong σ-bonds.[22,23] The low-basicity pyridines, on the other hand, are weak σ-donors but reasonable π-acceptors, as we have shown for the corresponding Fe(III) complexes,[22] and were expected to interact with the filled d_π orbitals of the low-spin d^6 metal to help stabilize the axial ligand bonds through $d_\pi-p_\pi$ back-bonding. For the bis-pyridine complexes of the present study, we must consider the question of why the symmetrical low-spin d^6 electron configuration of $[Fe^{II}TMP(L)_2]$ complexes prefer parallel alignment of identical planar axial ligands rather than perpendicular (independent of the question of ruffling), when the latter would allow, especially for low-basicity pyridines, π-back-bonding from one d_π orbital to the π^* orbital of one pyridine and a similar interaction from the other d_π orbital to the other pyridine. This expectation assumes that such π-back-bonding interactions provide large energies of stabilization in low-spin Fe(II) porphyrinates having two identical axial ligands. In fact, this may not be true, as suggested by the CO complexes of hemoglobin and myoglobin, and their models: There are, to our knowledge, no reports of stable bis-CO complexes of Fe(II) porphyrinates, but for the unsymmetrical axial ligand complexes where one ligand is a strong σ and π donor while the other is a weak σ donor and a strong π acceptor, the equilibrium constants for CO addition have been measured by several research groups, and are in the 10^7-10^9 M^{-1} range for simple iron(II) porphyrinates bound to imidazoles or pyridines,[69−71] many orders of magnitude larger than the equilibrium constants for adding a second identical nitrogenous base, K_2 ($\sim 10^2-10^4$ M^{-1}).[26] In the case of CO addition it could be argued that both σ donation from the lone pair and the filled-filled π interaction of the nitrogen donor ligand with the d_{xz} and d_{yz} orbitals of Fe(II) "fattens" these filled orbitals for π back-donation to the CO. Without the "push" of a strong σ and π donor ligand, Fe(II) shows little tendency to bind to strong π acceptor ligands (and it should be noted that Fe(III) should show even less, a conclusion that is consistent with the absence of any report of a CO complex of a Fe(III) porphyrinate). For two identical axial ligands, both have equal "push" and "pull", and hence the d_π orbitals of the d^6 low-spin Fe(II) center may be fairly passive in this case. In fact, for low-spin Fe(III) porphyrinates, what we had previously attributed to π back-donation from the d_π orbitals of Fe to the π^* orbitals of low-basicity pyridines or isonitriles may instead be a case of the smaller crystal field strength of these ligands (a σ bonding effect) as compared to high-basicity pyridines and imidazoles, that places the d_{xz},d_{yz} orbitals at lower energy than d_{xy} for weak σ-donor ligands.

The hypothesis of passivity is supported by recent Self-Consistent-Charge-Xα calculations in the Local Density Approximation (LDA) for two bis-imidazole complexes of Fe^{II}-TMP.[40] The complexes studied were $[Fe(TMP)(1\text{-MeIm})_2]$[72a] and $[Fe(TMP)(2\text{-MeHIm})_2]$.[72b] The results show that in both cases the d_{xy} orbital is higher in energy than the d_π orbitals, and that, as expected, the energy difference between d_{xz} and d_{yz} is very small for the hindered imidazole complex (perpendicular planes, 0.006 eV). But it is only slightly larger for the nonhindered imidazole complex (parallel planes, 0.018 eV). The population of the d_{xy} orbital is very similar for the two complexes (1.982 and 1.988, respectively), and is slightly larger than the population of d_{xz} (1.740 and 1.859, respectively) and d_{yz} (1.756 and 1.805, respectively), as predicted by the observed positive sign of the EFG found in the magnetic Mössbauer spectra.[40]

(67) Quinn, R.; Nappa, M.; Valetine, J. S. *J. Am. Chem. Soc.* **1992**, *104*, 2588.

(68) Walker, F. A. Unpublished results.

(69) El-Kasmi, D.; Tetreau, C.; Lavalette, D.; Momenteau, M. *J. Am. Chem. Soc.* **1995**, *117*, 6041 and references therein.

(70) Hashimoto, T.; Dyer, R. L.; Crossley, M.; Baldwin, J. E.; Basolo, F. *J. Am. Chem. Soc.* **1982**, *104*, 2101.

(71) Collman, J. P.; Brauman, J. I.; Iverson, B. L.; Sessler, J. L.; Morris, R. M.; Gibson, Q. H. *J. Am. Chem. Soc.* **1983**, *105*, 3052.

(72) (a) Structural parameters taken from $[Fe(TPP)(1\text{-BzylIm})_2]$.[31] (b) Structural parameters taken from $[Fe(TMP)(1,2\text{-}Me_2Im)_2]ClO_4$.[23]

The latter two orbital populations are, in fact, smaller for the case of perpendicular as compared to parallel ligands, as predicted in the Mössbauer section above, but the difference is small. The population of $d_{x^2-y^2}$ is also greater for the case of perpendicular ligands than for parallel (0.584 and 0.500, respectively), and greater than the population of d_{z^2} in both cases (0.479 and 0.438, respectively), and this population difference also contributes to the positive electric field gradient found in the magnetic Mössbauer spectra.[40] Thus, based upon orbital populations, both porphyrin and axial ligand σ donor and metal π back-bonding interactions are calculated to be slightly greater in the case of perpendicularly-aligned axial ligands, but these effects are believed to be due mainly to the shorter N_P-Fe bonds that result from ruffling of the porphyrinate ring.[40]

The energy difference between the filled "$e_g(\pi)$" orbitals is calculated to be smaller for the hindered (0.039 eV) than for the nonhindered imidazole complex (0.074 eV), although these orbitals contain only 2% metal 3d character.[40] However, more interesting than the filled orbital energies is the difference in energy of the LUMO "$e_g(\pi^*)$" orbitals, which is small (0.006 eV) for the case of ligands in perpendicular planes and quite large (0.168 eV) for the case of ligands in parallel planes, even though the percent Fe(3d) character is small in both cases (6−10%) (although slightly larger for the case of perpendicular ligands (9, 10%) than for parallel (6, 7%)). It is also interesting to note that the percent Fe(3d) character is similar for both "$e_g(\pi^*)$" orbitals in each case, in spite of the fact that for the case of parallel planes, the ligand π and π^* orbitals can mix with one metal d_π orbital and not the other. Thus, the effect upon the energies of the porphyrin π^* LUMO orbitals for the case of parallel ligands is much greater than that upon the d_π orbitals of the metal, and the metal d character of the π^* LUMO orbitals is fairly small, suggesting that the metal orbitals of low-spin Fe(II) are, for the most part, noninteracting—they may well funnel information from the axial ligands to the porphyrinate π system but are of themselves not very much affected by axial ligand plane orientation.

Summary and Conclusions. From the above discussion of bonding interactions it has become apparent that they do not explain the observed stabilization of parallel ligand orientation in Fe(II) porphyrinates, and to understand the reasons for this stabilization we must focus on the porphyrinate ring, in particular on the energetics of ruffling for low-spin d^6 as compared to low-spin d^5 systems. In the case of low-spin Fe(III) porphyrinates the d_π orbitals *appear* to interact with the axial ligands; the strongest evidence for this is the extreme ruffling of [Fe(TPP)(*t*-BuNC)$_2$]ClO_4 and [Fe(OEP)(*t*-BuNC)$_2$]ClO_4,[64] where there is no *structural* reason for the ruffling, but rather an *electronic* reason, to stabilize the $(d_{xz},d_{yz})^4(d_{xy})^1$ electronic configuration by porphyrin→Fe(III) π donation, as discussed above and elsewhere[55] for [Fe(TPP)(4-CNPy)$_2$]ClO_4. However, as suggested above, rather than π donation from the d_π orbitals to the axial ligands, it may be that the weak σ-donor strength of isonitriles and low-basicity pyridines is actually responsible for placing d_{xy} at higher energy than the d_π orbitals, and this electron configuration is then stabilized in the low-spin Fe(III) case by ruffling. It is interesting to note that in the iron(II) derivative, [Fe(TPP)(*t*-BuNC)$_2$],[73] the porphinato core is only very slightly saddled. What is quite apparent from the present study is that a major difference between the low-spin d^5 and d^6 electron configurations is that complete filling of the three d_π orbitals of octahedral symmetry removes the possibility of porphyrin→Fe π donation, and thereby removes any *electronic* reason for ruffling. This is important for the $(d_{xz},d_{yz})^4(d_{xy})^2$ configuration of complexes of this study,[40] in comparison to the Fe(III) cases mentioned above, where only one electron is in the d_{xy} orbital, and Por→Fe(III) π donation from the $a_{2u}(\pi)$ orbital *requires* ruffling.[55,64]

It thus appears that the low-spin d^6 electronic configuration finds no stabilization due to ruffling of the porphyrinate ring and, in fact, is *destabilized* by ruffling, if the nearly two orders of magnitude lower stability of [Fe(TMP)(2-MeHIm)$_2$] than of [Fe(TMP)(1-MeIm)$_2$] (Table 10) is considered. This difference in complex stability alone amounts to a free energy difference of 10.3 kJ/mol at 298 K. In comparison, for the Fe(III) analogs of Table 10, the free energy difference is only 2.9 kJ/mol. The difference between these two free energy differences, 7.4 kJ/mol, may be thought of as a measure of the effect of the difference in electron configuration of the two oxidation states, assuming that the Fe(III) and Fe(II) derivatives have very similar geometries.[8,40] To this 7.4 kJ/mol we must now add the energy required to ruffle the porphyrinate ring for the Fe(II) complex (with its axial ligands in perpendicular planes), which has been cancelled out in this $\Delta\Delta G$ calculation. Although we do not have a direct measure of the ΔG of ruffling, we have calculated the ΔH of ruffling of the TMP ring by MM2 methods.[55] Assuming that the value obtained, 4 kJ/mol for [Fe^{III}(TMP)(Py)$_2$]$^+$,[55] is similar for the Fe(II) analog, and that the entropy of ruffling is small, we can expect the barrier to ruffling of the porphyrinate ring (and thus placing planar ligands in perpendicular planes) will be at least another 4 kJ/mol higher. Thus, it appears that the stabilization free energy of the parallel (planar ring) over perpendicular (ruffled ring) structures of low-spin Fe(II) porphyrinates may be of the order of at least −11.4 kJ/mol, a sizable stabilization for the parallel alignment of axial ligands.

Acknowledgment. We thank the reviewers of this paper for helpful comments and the National Institutes of Health for support of this research under Grant Nos. GM-38401 (W.R.S.), DK-31038 (F.A.W.), and GM-16406 (P.G.D.).

Supporting Information Available: Table S1, complete crystal data and intensity collection parameters; Tables S2−S4, final atomic coordinates for [Fe(TMP)(4-CNPy)$_2$], [Fe(TMP)(3-CNPy)$_2$], and [Fe(TMP)(4-MePy)$_2$], respectively; Tables S5−S8, hydrogen atom fractional coordinates and isotropic thermal parameters, anisotropic thermal parameters, group parameters for the chloroform solvent, and fractional coordinates for the fixed chloroform solvent for [Fe-(TMP)(4-CNPy)$_2$]; Tables S9 and S10, hydrogen atom fractional coordinates and isotropic thermal parameters, and anisotropic thermal parameters for [Fe(TMP)(3-CNPy)$_2$]; and Tables S11 and S12, hydrogen atom fractional coordinates and isotropic thermal parameters, and anisotropic thermal parameters for [Fe(TMP)(4-MePy)$_2$] (17 pages). See any current masthead page for ordering and Internet access instructions.

JA9715657

(73) Jameson, G. B.; Ibers, J. A. *Inorg. Chem.* **1979**, *18*, 1200.